Multi-point Wind Power Injection for Mitigation of Inter-area Oscillation in Smart Grids

Syed Z. Rizvi and Javad Mohammadpour
College of Engineering, The University of Georgia, Athens, GA 30602, USA
Emails: {szrizvi, javadm}@uga.edu

***Abstract*—This work investigates inter-area oscillation in large-scale wind-integrated power grids when wind power is injected from multiple wind farms located at different locations. Previous results in the literature have shown that the location of wind power injection is detrimental to the frequency response of inter-connected generators. In this work, we seek to find an optimal wind-power injection location leading to the most desirable power spectrum. However, owing to meteorological, weather and economic conditions, it is not always possible to site a wind farm or grid connection point at the desired location. We then present a controller design method so that a power system with wind farms at other locations can obtain a frequency response matching the response of a system having farms at the desired location. Numerical examples with multiple wind farms are simulated and it is shown that injecting power from multiple wind farms significantly improves the desired frequency response matching.**

I. Introduction

With the research in wind energy gaining momentum, there has been a consistent increase in the amount of wind power penetration over the last decade. According to the American Wind Energy Association (AWEA), as of the first quarter of 2013, the cumulative installed capacity of wind power generation in the US has been brought to 60,009 MW [1], with total wind power penetration in the US standing at 3.67% of all generated electrical energy [2]. This growing integration of wind power in the power grids has brought challenges to several aspects of power system operations such as transient stability, protection, and voltage stability and control [3], [4]. One such aspect is the impact of wind power on the inter-area electromechanical oscillations. Inter-area oscillations occur when a group of coherent generators in a certain area of power network starts oscillating against another coherent group in another area of the network [3]. These oscillations generally have a frequency range of 0.1 to 0.9 Hz [3], [5].

Of the many aspects that affect inter-area oscillation, the location of a wind farm is an important factor [5]. Often, siting or connecting a wind farm to the grid at a specific location might not be feasible due to reasons that range from economic and geographical to meteorological. By considering the power system as a continuum and modeling it in terms of a linear partial differential equation in [6], an attempt was made in [5] to design a control strategy for a power grid with a single wind turbine so that the frequency response of the inter-area oscillation matches the desired response over a small frequency range. This controller performance was observed to deteriorate as the optimization frequency range was increased.

TABLE I: Nomenclature of variables

Variable	Description
δ_i	Rotor angle for i^{th} machine [rad]
x_i	Reactance between machines i and $i+1$ [Ω]
γ	Impedance density [Ω/unit distance]
$P_{gi}(t)$	Power generated by i^{th} wind farm [W]
$W(u,t)$	Total wind power [W]
α	normalized wind farm location $\in$ [0,1]
α_d	desired normalized wind farm location $\in$ [0,1]
V	wind farm controller parameters
k_n	wave number [rad/m]
ω	frequency [rad/s]
ν	wave speed [m/s]
Sp	power spectrum [dB]
λ	wind turbine tip-speed ratio
C_P	wind turbine power coefficient [0-100%]
β	wind turbine blade pitch angle [deg]
ϕ	wind turbine lumped input parameter

In the present paper, we take a step further and investigate the effects of increased wind power penetration when power is injected from multiple farms located at different locations. We note that by considering a more realistic scenario of multi-point wind power injection, an improvement is observed in terms of the controller performance over a wider frequency band. We also investigate how to select a desired power injection location. A nomenclature of variables used for different notations in the paper has been tabulated in Table I. The paper is arranged as follows. Section II takes a look at power system model, spectrum analysis and the control objectives. Section III discusses the design method for finding the desired power injection location and controller parameters. Numerical examples with single and multiple wind turbines are considered and the results are discussed in Section IV. Finally, based on the presented results, some concluding remarks are made in Section V.

II. Problem Statement

A simple approach to model the dynamic characteristics of a large power network is to visualize the system as being spread out until it becomes a continuum. Such a model is capable of describing low frequency modes for a system having large number of machines with a reasonable accuracy [6]. Consider

978-1-4799-3653-3/14/$31.00 ©2014 IEEE

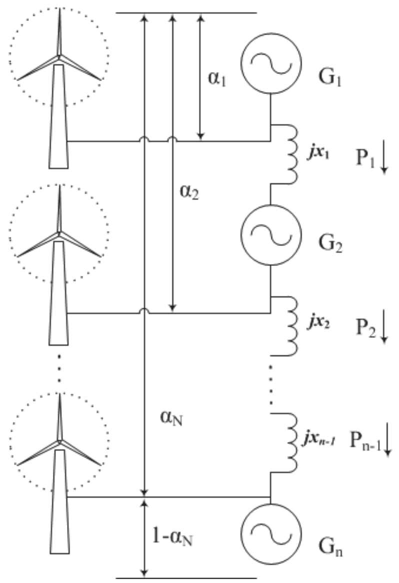

Fig. 1: A network of generators with multiple wind farms injecting power at different locations

a string of generators as shown in Figure 1. Variables G_i and δ_i represent the generation and rotor angle for i^{th} machine, and P_i and x_i are change in power and effective reactance between the machines i and $i+1$, respectively. Variable u is an arbitrary distance. The equation of motion for the i^{th} machine is given by

$$\left(\frac{2H}{377}\right) G_i \frac{d^2\delta_i}{dt^2} = P_{i-1} - P_i, \quad (1)$$

where H is the moment of inertia constant for each generator. As shown in [6], the expression for change in power between machines i and $i+1$ can therefore be written as

$$P_i = \frac{\delta_i - \delta_{i+1}}{x_i} = \frac{1}{x_i/\Delta u} \cdot \frac{\delta_i - \delta_{i+1}}{\Delta u}. \quad (2)$$

This gives the following relation for the system power flow when $\Delta u \to 0$ and assuming impedance to be continuously distributed [6]:

$$p\ (u,t) = -\frac{1}{\gamma} \cdot \frac{\partial \delta(u,t)}{\partial u}, \quad (3)$$

where $\gamma = \frac{dx(u)}{du}$ is the impedance density. Formulating a similar expression for p_{i-1} and substituting in (1), gives the following when divided by Δu on both sides:

$$\frac{1}{\gamma}\frac{\partial^2\delta(u,t)}{\partial u^2} = \left(\frac{2H}{377}\right)\frac{dG(u)}{du} \cdot \frac{\partial^2\delta(u,t)}{\partial t^2}. \quad (4)$$

The term $P_T = \frac{dG(u)}{du}$ is known as the generation density. Lumping the constants together gives us the expression for wave speed $\nu = \left(\frac{377}{2HP_T\gamma}\right)^{1/2}$, leading to the relation [6]

$$\frac{\partial^2\delta(u,t)}{\partial t^2} - \nu^2\frac{\partial^2\delta(u,t)}{\partial u^2} = 0. \quad (5)$$

Adding a damping term, and considering multiple sources of power from N wind farms, the equation above can be written as

$$\frac{\partial^2\delta(u,t)}{\partial t^2} + \zeta\frac{\partial\delta(u,t)}{\partial t} - \nu^2\frac{\partial^2\delta(u,t)}{\partial u^2} = W(u,t), \quad (6)$$

where $W(u,t)$ is the net injected wind power.

A. Analyzing the Power Spectrum

If the wind farm i is connected to the grid at location α_i normalized over $[0,1]$ along the path of the generators, $W(u,t)$ can be expressed as

$$W(u,t) = \sum_{i=1}^{N} P_{gi}(t)\hat{\delta}(u-\alpha_i), \quad (7)$$

where $P_{gi}(t)$ is the power generated and injected by the wind farm i, and $\hat{\delta}$ is the dirac-delta function indicating point-source injection. In order to solve (6), $\delta(u,t)$ and wind power $W(u,t)$ are represented in terms of their Fourier series as

$$\delta(u,t) = \frac{1}{2}A_0(t) + \sum_{n=1}^{\infty}(A_n(t)cos(k_n u) + B_n(t)sin(k_n u)), \quad (8)$$

$$W(u,t) = \frac{1}{2}F_0(t) + \sum_{n=1}^{\infty}(F_n(t)cos(k_n u) + G_n(t)sin(k_n u)), \quad (9)$$

where k_n is the wave number of the n^{th} node, which can be approximated by $n\pi$ [6]. This gives us the boundary conditions

$$p(0,t) = p(1,t) = 0, \quad (10)$$

which implies a standing wave with zero slope at $u=0$ and $u=1$. Using this boundary condition, $B_n(t)$ and $G_n(t)$ would vanish and the wave equation is reduced to the following ordinary differential equation

$$\frac{d^2A_n(t)}{dt^2} + \zeta\frac{dA_n(t)}{dt} + k_n^2\nu^2A_n(t) = F_n(t). \quad (11)$$

Using (7), $F_n(t)$ can be written as

$$F_n(t) = \int_0^1 cos(k_n u)W(u,t)du = 2\sum_{i=1}^{N} P_{g_i}(t)cos(k_n\alpha_i). \quad (12)$$

Using (12) in (11) and taking Laplace transform results in

$$A_n(\omega,\alpha) = \sum_{i=1}^{N}\frac{2P_{g_i}cos(k_n\alpha_i)}{(\nu^2k_n^2-\omega^2) + \mathbf{j}\ (\zeta\omega)},$$

where $\alpha = [\alpha_1 \ \cdots \ \alpha_N]$ is the set of available power-injection points for the wind farms. Power spectrum of A_n can now be derived as

$$S_{A_n}(\omega,\alpha) = 4\sum_{i=1}^{N} S_{pg_i}f_i(\omega,\alpha_i) + 2\sum_{j=1}^{N-1}\sum_{l=j+1}^{N}(S_{pg_{j,l}})\ f_j(\omega,\alpha_j)f_l(\omega,\alpha_l),$$

where

$$f_i(\omega, \alpha_i) = \frac{cos^2(k_n \alpha_i)}{(k_n^2 \nu^2 - \omega^2)^2 + \zeta^2 \omega^2}. \quad (13)$$

Since $j \neq l$ in $(S_{pg_{j,l}})$, we can neglect the last summand due to the uncorrelated spectra. This gives us the spectrum

$$S_{A_n}(\omega, \alpha) = 4 \sum_{i=1}^{N} S_{pg_i} f_i(\omega, \alpha_i). \quad (14)$$

Using (3) and the boundary conditions (10), we have

$$p(u,t) = \frac{1}{\gamma} \sum_{n=1}^{\infty} A_n(t) k_n sin(k_n u). \quad (15)$$

Consequently, we can obtain the power spectral density as

$$Sp\ (\omega, \alpha) = \frac{1}{\gamma^2} \sum_{n=1}^{\infty} S_{A_n}(\omega, \alpha) k_n^2 sin^2(k_n u). \quad (16)$$

Using (14) in (16), we determine

$$Sp\ (\omega, \alpha) = \frac{4}{\gamma^2} \sum_{i=1}^{N} S_{pg_i}(\omega) \sum_{n=1}^{\infty} \frac{k_n^2 cos^2(k_n \alpha_i) sin^2(k_n u)}{(k_n^2 \nu^2 - \omega^2)^2 + \zeta^2 \omega^2}. \quad (17)$$

Having defined the spectrum, the problem is stated as:

Find a desired injection point α_d and design wind farm controllers, such that the spectrum of system with closed-loop wind farms matches that with a system having wind farms connected at α_d.

III. Controller Design and Optimization Procedure

The nonlinear lumped-parameter model of a wind turbine consists of different subsystem models. This includes the *aerodynamic model*, the *drive-train model*, *electrical system model*, and the *pitch actuator model*. We use the three degree-of-freedom (3-DOF) lumped-parameter model first presented in [7]. Due to space limitation, we do not describe the model here, and refer the interested reader to [7], [8].

Control of wind turbines usually involves control of generator torque T_g or blade pitch β depending upon the region of operation defined by the wind speed v_ω. In this work, similar to [5], we will use a linearized model of the wind turbine's lumped-parameter model. Block diagram of a closed-loop wind turbine is shown in Figure 2, with $H(s)$ denoting a feedback controller and $G(s)$ denoting the linearized wind turbine model. We define the wind turbine control input as $\phi = \frac{1}{\omega_r(t)} v_\omega^3(t) C_P(t)$ similar to previous work [5], where ω_r is the turbine rotor speed and v_ω and $C_P(t)$ are the wind speed and the power coefficient of the wind turbine, respectively. The selected control input ϕ essentially lumps the nonlinear terms in the system model and leads to a linear state-space form for the wind turbine dynamics. In order to employ torque or pitch control, consider the tip-speed ratio λ of the wind turbine defined as

$$\lambda = \frac{r\omega_r}{v_\omega}, \quad (18)$$

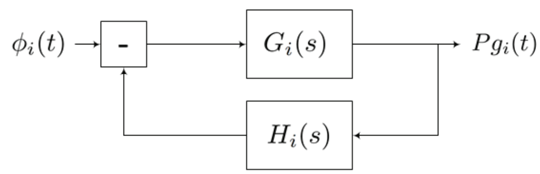

Fig. 2: Configuration of the closed-loop system for i^{th} wind turbine

where r is the radius of the swept area of the wind turbine blades. The power and torque coefficients are related through

$$C_P(\beta, \lambda) = C_Q(\beta, \lambda)\ \lambda = \frac{C_Q(\beta, \lambda) r \omega_r}{v_\omega}.$$

Substituting (19) in ϕ results in

$$\phi = \frac{1}{\omega_r} v_\omega^3 C_P(\beta, \lambda) = v_\omega^2 C_Q(\beta, \lambda) r.$$

Hence, if ϕ is known, pitch angle β can be found from the torque coefficient look-up table. Since $C_Q(\beta, \lambda)$ depends highly nonlinearly on both the pitch angle β and the tip-speed ratio λ, changing the control input from ϕ to β makes the control problem a bit more challenging. For the simplicity of the control design, we retain ϕ as the control input. Controller $H(s)$ is considered to be a simple controller with one zero and two poles represented by

$$H(s) = \frac{c_{n_1} s + c_{n_0}}{c_{d_2} s^2 + c_{d_1} s + c_{d_0}}. \quad (19)$$

The above control structure was selected through a trial-and-error process to guarantee the design specifications and also the simplicity of the controller implementation. Power spectrum with power injection from controlled wind turbines can be written as

$$Sp_{cl}(\omega, \alpha, V) = \frac{4}{\gamma^2} \sum_{i=1}^{N} S_{pg_i}^{\,cl}(\omega, V) \sum_{n=1}^{\infty} \frac{k_n^2 cos^2(k_n \alpha_i) sin^2(k_n u)}{(k_n^2 \nu^2 - \omega^2)^2 + \zeta^2 \omega^2}, \quad (20)$$

where $S_{pg_i}^{\,cl}$ denotes power spectrum of the closed-loop wind turbine i. The design problem is to find a desired power injection location α_d and controller parameters V for the respective wind turbines in order to match the power spectrum of a system having wind turbines connected at other locations with that of a system having wind turbines connected at α_d. We pose this problem as an *integrated nonlinear optimization* problem. The objective function can be represented as follows:

$$\begin{aligned} J &= \underset{\alpha_d,\, V}{\operatorname{argmin}}\, W_1 \int_{\omega_1}^{\omega_2} \Big[Sp^{\ dB}(\alpha_d, \omega)\Big]^2 d\omega \\ &+ \underbrace{W_2 \int_{\omega_1}^{\omega_2} \Big[Sp_{cl}^{dB}(\alpha, \omega, V) - Sp^{\ dB}(\alpha_d, \omega)\Big]^2 d\omega}_{\Phi}, \end{aligned} \quad (21)$$

where W_1 and W_2 are weighting coefficients and $Sp^{\ dB}$ and Sp_{cl}^{dB} are the power spectrum in decibel with open and closed-loop wind turbines, respectively. The first term pertains to

TABLE II: Optimized parameter values for frequency range $[\omega_1, \omega_2]$. Parameter V consists of the coefficients of the controller (19)

Wind Turbines	$[\omega_1, \omega_2]$	$\alpha_{1,2}$	α_d	V	Mismatch (Φ)
1	[0.1,0.2]	$\alpha_1 = 0.15$	0.73	$V_1 = [7.36\ 0.01\ 0.01\ 5.74\ 10.2]$	0.432
2	[0.1,0.2]	$\alpha_1 = 0.15$, $\alpha_2 = 0.62$	0.73	$V_1 = [15.02\ 0.27\ 0.56\ 5.57\ 3.11]$, $V_2 = [0.10\ 2.72\ 2.43\ 3.29\ 5.20]$	7.95×10^{-5}
1	[0.1,0.7]	$\alpha_1 = 0.15$	0.59	$V_1 = [45.95\ 2.55\ 1.38\ 2.62\ 4.49]$	6.46
2	[0.1,0.7]	$\alpha_1 = 0.15$, $\alpha_2 = 0.62$	0.59	$V_1 = [78.31\ 0.10\ 6\ 4.42\ 13.5]$, $V_2 = [12\ 0.10\ 5.08\ 3.39\ 36.38]$	0.29

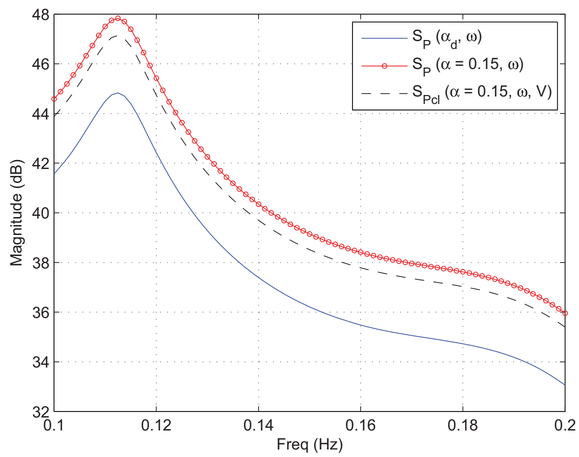

Fig. 3: Power spectrum with power injection from one wind farm optimized for [0.1,0.2] Hz

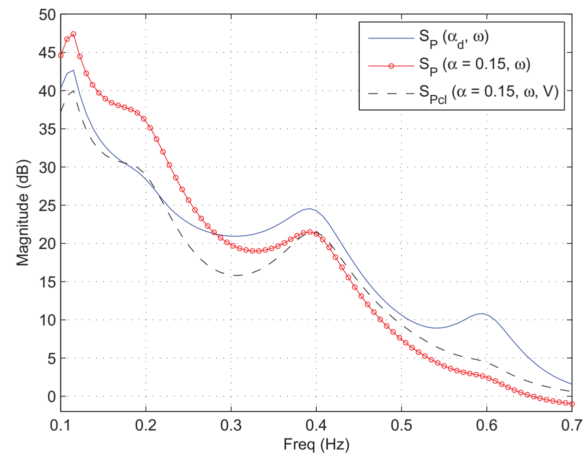

Fig. 5: Power spectrum with power injection from one wind farm optimized for [0.1,0.7] Hz

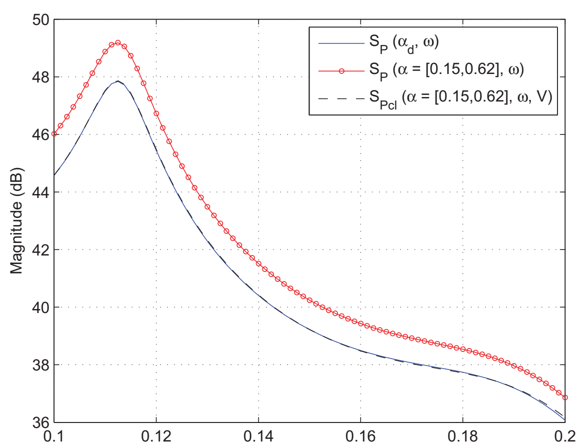

Fig. 4: Power spectrum with power injection from two wind farms optimized for [0.1,0.2] Hz

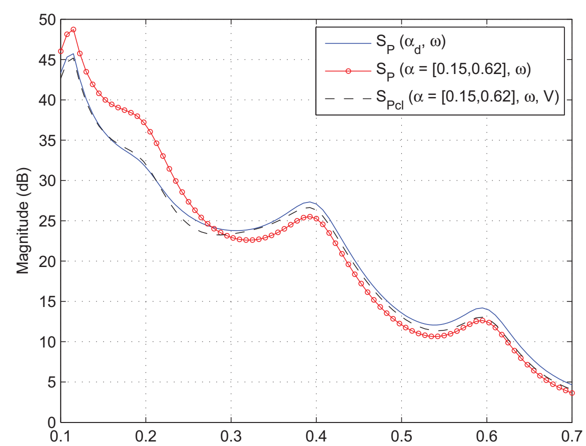

Fig. 6: Power spectrum with power injection from two wind farms optimized for [0.1,0.7] Hz

finding a desired power injection point and seeks to find α_d that minimizes the overall area under the power spectrum curve. Other formulations like minimizing infinity norm of the spectrum can be suggested if one wishes to minimize the mode peaks. The second term seeks to minimize the mismatch between the controlled and desired response. The rationale behind our integrated design is to find the most desired power injection point α_d that minimizes the low-frequency inter-area oscillation, and a controller that is able to match that desired response.

IV. Simulation Results and Discussion

We determine the power spectra (17) and (20), which are associated with open and closed-loop wind turbines, respectively. Detailed parameter values for the NREL 5MW wind turbine were taken from [8] and the final linearized model computed in [5] was used as

$$G(s) = \frac{6.786s + 1.939e^4}{s^3 + 0.294s^2 + 816.2s + 0.7696}. \quad (22)$$

We then solve the underlying optimization problems for cases with one and two wind turbines. Optimized values of the desired injection point α_d, controller parameters V and mismatch Φ for each case are tabulated in Table II. Mismatch Φ is the second term of the cost function J as indicated in (21). We generated different initial conditions randomly and ran Monte-Carlo simulations. Optimization was carried out using interior-point methods, as well as heuristic search techniques. It was assumed that the wind turbines can be connected to the grid at $\alpha = 0.15$ and $\alpha_{1,2} = 0.15, 0.62$ for the single and two-point injection cases, respectively. As mentioned earlier, α is a normalized distance along the path of the generators and has a value in the range $[0, 1]$. Control parameters are first optimized for $[0.1, 0.2]$ Hz. A desired injection point $\alpha_d = 0.73$ is obtained for both cases. The spectra are shown in figures 3 and 4 that exhibit a greater matching between desired (solid line) and controlled (dotted line) spectra for two-point injection case. This can also be gauged from the value of Φ for the two cases listed in Table II. The resulting closed-loop wind turbines have all the eigenvalues in the left half side of the s-plane. As mentioned earlier, the frequency response matching is known to deteriorate for wider frequency bands. However, with multi-point wind power injection, we observe encouraging results with controllers optimized for $[0.1, 0.7]$ Hz. Results for single and two-point injection are shown in figures 5 and 6, respectively. It should be noted that the available locations of wind power injection $\alpha_{1,2}$ were simply assumed. Similar results were achieved when different values of $\alpha_{1,2}$ were assumed randomly.

Since wind power injection, in this study, acts as an external disturbance to the grid, a tradeoff exists between frequency response matching and power production. A better frequency response matching translates to more wind-power attenuation in the low frequency range and hence lesser power production by the wind turbine. This can be seen in the step responses in Figure 7, where a greater frequency response matching for [0.1,0.2] Hz accounts for a lower magnitude in the time-simulation. For these time simulations, wind speed of $v_\omega = 8m/s$ was considered, which corresponds to region 2 wind turbine control with values $\lambda_{opt} = 7.55$, $C_{P_{max}} = 0.482$, and $\omega_r = 0.9587rad/s$ for the NREL 5MW wind turbine [9]. This gives us $\phi = \frac{1}{\omega_r} v_\omega^3 C_P(t) = 257.41$. To further the balance between spectrum matching and power production, more constraints can be imposed and additional terms can be added to the cost function for power production maximization.

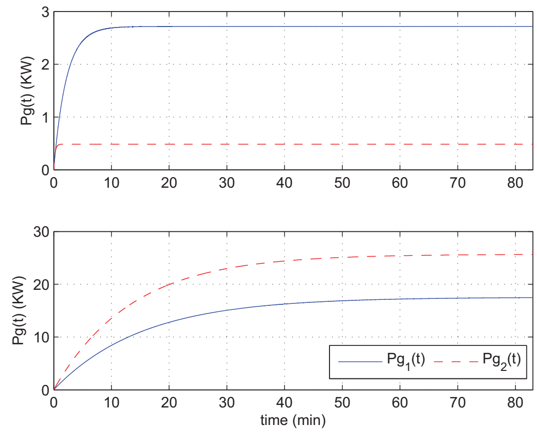

Fig. 7: Step-response of the two closed-loop wind turbines optimized for [0.1,0.2] Hz (top) and [0.1,0.7] Hz (bottom)

V. Concluding Remarks

In this work, we examined a realistic scenario for mitigating inter-area oscillation in wind-integrated power grids when wind power is injected from multiple wind farms at different spatial locations. Previous results had shown that with wind power injected from a wind farm, desired frequency response could be achieved over a small frequency range. We made an attempt to extend the previous work by finding the desired power injection point and matching the desired frequency response when wind power is injected from multiples sites. A subject of our ongoing research is to extend this work to a more realistic nonlinear or linear-parameterized wind turbine model from the pitch angle β to generated power $P_g(t)$, instead of a linearized wind turbine model from a lumped control input ϕ to $P_g(t)$.

References

[1] "U.S. Wind Industry First Quarter 2013 Market Report," Amer. Wind Energy Assoc., Washington, DC, Apr. 2013.

[2] "Electric Power Monthly with data for April 2013," U.S. Dept. of Energy, Energy Info. Administration, Washington, DC, Jun. 2013.

[3] J.G. Slootweg and W.L. Kling, "The impact of large scale wind power generation on power system oscillations," *Elect. Power Syst. Res.*, vol. 67, pp. 9-20, 2003.

[4] J.G. Slootweg, S.W.H. de Haan, H. Polinder, and W.L. Kling, "Voltage control methods with grid connected wind turbines: a tutorial review," *Wind Engineering*, vol. 25, no. 6, pp. 353-365, 2001.

[5] D.F. Gayme and A. Chakrabortty, "Shaping power system inter-area oscillations through control loops of grid integrated wind farms," in *51st IEEE Conference on Decision & Control*, Maui, HI, pp. 2012, 5004-5009.

[6] R. L. Cresap and J. F. Hauer, "Emergence of a new swing mode in the western power system," *IEEE Trans. Power App. Syst.*, vol. PAS-100, no. 4, pp. 2037-2045, Apr. 1981.

[7] F.D. Bianchi, H. De Battista, and R.J. Mantz, *Wind Turbine Control Systems: Principles, Modelling and Gain Scheduling Design, Advances in Industrial Control*. London: Springer, 2006.

[8] C. Sloth, T. Esbensen, and J. Stoustrup, "Active and passive fault-tolerant LPV control of wind turbines," in *American Control Conf.,* Baltimore, MD, 2010, pp. 4640-4646.

[9] J. Jonkman, S. Butterfield, W. Musial, and G. Scott, "Definition of a 5-MW reference wind turbine for offshore system development," National Renewable Energy Lab., Golden, CO, Tech. Rep. NREL/TP-500-38060, Feb. 2009.